Experimental and computational study on thermoelectric generators using thermosyphons with phase change as heat exchangers

M. Araiz[a], A. Martínez[a,b,*], D. Astrain[a,b], P. Aranguren[a,b]

[a] Mechanical, Energy and Materials Engineering Department, Public University of Navarre, 31006 Pamplona, Spain

[b] Smart Cities Institute, Pamplona, Spain

*Corresponding author Tel.: +34 948 16 9309; fax: +34 948 169099

E-mail address: alvaro.martinez@unavarra.es (A. Martinez)

Abstract

An important issue in thermoelectric generators is the thermal design since it can really improve their performance by increasing the heat absorbed or dissipated. Due to its several advantages, compared to conventional dissipation systems, this work proposes a thermosyphon heat exchanger with phase change to be place on the cold side of thermoelectric generators. Some of these advantages are: high heat-transfer rates; absence of moving parts and lack of auxiliary consumption (because fans or pumps are not required); and the fact that these systems are wickless. This work presents a computational model developed to design and predict the behaviour of this heat exchangers. Furthermore, a prototype has been built and tested in order to demonstrate its performance and validate the computational model. It turns out that the model predicts the thermal resistance of the heat exchanger with a relative error in the interval [-8.09; 7.83] percent in the 95% of the cases. Finally, the use of thermosyphons with phase change in thermoelectric generators has been studied in a waste-heat recovery application, stating that including them on the cold side of the generators improves the net thermoelectric production by 36 % compared to that obtained with finned dissipators under forced convection.

Keywords

computational model; thermosyphon with phase change; thermoelectric generator; waste-heat recovery

Nomenclature

A_b	Base area of the evaporator (m²)
A_{im}	Base area of the interface material (m²)
A_m	Base area of one thermoelectric module (m²)
Bi	Biot number
b_i	Systematic uncertainty for the experimental variable *i*
c_{pl}	Liquid specific heat capacity (J/kgK)
d_e	Tube external diameter (m)
d_i	Tube inside diameter (m)
D	Equivalent fin diameter (m)
e	Wall's evaporator's base thickness (m)
e_{im}	Interface material thickness (m)
g	Acceleration due to gravity (m/s²)
h_b	Boiling heat transfer coefficient (W/m²K)
h_{cI}	Condensation heat transfer coefficient with turbulent flow (W/m²K)
h_{cII}	Condensation heat transfer coefficient with laminar flow (W/m²K)
H	Fin height (m)
I_{ps}	Electric current supplied to the electric resistances (A)
i_{lg}	Latent heat of vaporization (J/kg)
k_{Al}	Thermal conductivity of the aluminium (W/mK)

k_{im}	Thermal conductivity of the interface material (W/mK)
k_l	Liquid thermal conductivity (W/mK)
L	Condensation tube's length (m)
N	Number of thermoelectric modules
Nu	Nusselt number
P_{max}	Maximum electric power generated with TEG (W)
p_r	Reduced pressure (P/P_c)
Pr_l	Prandtl number
$\dot{Q}_c$	Heat flux dissipated by the heat exchanger (W)
R_b	Boiling thermal resistance (K/W)
R_c	Condensation thermal resistance (K/W)
R_{cold}	Thermal resistance of the cold side of the TEG (K/W)
R_{cond_b}	Conduction thermal resistance through the evaporator's base (K/W)
R_{cond_t}	Conduction thermal resistance through the condensation tubes' wall (K/W)
R_{const}	Constriction thermal resistance (K/W)
R_{cont}	Contact thermal resistance (K/W)
R_{conv}	Natural convection thermal resistance (K/W)
R_{HE}	Thermal resistance of heat exchanger per module (K/W)
R_{hot}	Thermal resistance of the hot side of the TEG (K/W)
Ra	Rayleigh number
Re_{LT}	Reynolds number assuming total mass flowing as liquid
Re_{LS}	Reynolds number assuming liquid phase flowing alone
T_{amb}	Ambient temperature (K)
T_c	Temperature on the cold side of the thermoelectric modules (K)
$T_{out}^{wall}, T_{in}^{wall}$	Outside and inside evaporator's wall temperature (K)
$T_{out}^{tube}, T_{in}^{tube}$	Outside and inside tube's wall temperature (K)

T_{sat}	Saturation temperature (K)
V_{ps}	Voltage supplied to the electric resistances (V)
x	Vapour quality

Greek symbols

α	Thermal diffusivity (m²/s)
ΔP_{sat}	Difference in saturation pressure corresponding to ΔT_{sat} (Pa)
ΔT_{sat}	Difference between wall and saturation temperature (K)
β	Coefficient of thermal expansion (K^{-1})
γ	Parameter given by Eq. (13)
δ	Occupancy ratio
ϵ	Dimensionless contact radius, $\sqrt{\delta}$
λ_c	Empirical parameter given by Eq. (5)
μ_g	Gas viscosity (Ns/m²)
μ_l	Liquid viscosity (Ns/m²)
ν	Kinematic viscosity (m²/s)
ρ_g	Gas density (kg/m³)
ρ_l	Liquid density (kg/m³)
σ	Surface tension (N/m)
τ	Dimensionless wall thickness, $e/\sqrt{A_b \pi}$
Ψ	Dimensionless constriction thermal resistance

1. Introduction

The current energy situation, characterised by an increase in the energy consumption and the dependency on fossil fuels, has led several researches in order to improve the efficiency of the processes or to develop different ways for energy production, using, for instance, renewable sources. In this sense, thermoelectric generators (TEGs) can be used to produce electric energy from waste heat that, in other case, would be released to the ambient. This would increase the efficiency while using a free source of energy.

TEGs are made up of thermoelectric modules (TEM) based on the Seebeck effect, which are in charge of the transformation of heat into electricity; and heat exchangers, whose aim is to improve the efficiency of these devices. These exchangers have as purpose the reduction of the thermal resistances between the heat source and the hot side of the thermoelectric modules as well as that between the cold side of the modules and the ambient. In this way, the temperature difference between the hot and the cold side of the thermoelectric modules gets close to the maximum temperature gradient possible, which is the temperature difference between the heat source and the ambient, increasing the efficiency of the generator. The need to reduce these thermal resistances and to optimize the design of heat exchangers has been already proven [1,2].

A wide range of heat exchangers can be placed at the cold side of the modules in order to reduce the thermal resistance between this cold side and the ambient. Finned heat sinks are extensively used due to their simplicity as well as their relative low cost compared to other kind of heat exchangers. Working as active cooling systems, these dissipators can reach high cooling power rates [3–5]. Other kind of heat exchangers are the ones based on a liquid, such as water [6,7], which increase the performance of the system as they have higher convective coefficients. In these cases, there is an auxiliary consumption due to the electric power required to feed both the fans that make the air pass through the fins or the pumps that move the liquid inside the system [8].

Nowadays, there is a deep research in heat exchangers with phase change that improve heat transfer even more, with a small temperature drop, due to the use of the latent heat of an internal

fluid [9]. Heat pipes are the most common dissipators used of this range. They have an evaporator in contact with the cold side of the TEMs to absorb the heat that needs to be dissipated. This absorbed heat evaporates the fluid inside, which flows up to the condenser. Once up there, it condensates, as it releases the heat to the ambient, and it returns back to the evaporator. Some TEGs applications use heat pipes with a fan to help the heat to be transferred from the condenser to the ambient [10] whereas others take advantage of the free convection to remove the fan auxiliary consumption [11]. In both cases, fluid flow is achieved without pumps just by capillary effect of the wick which is inside the evaporator. This allows a heat pipe to work in any orientation but introduces two drawbacks: the capillary pressure caused by the wick may not be enough to pump the liquid back to the evaporator and an extra thermal resistance must be taken into account due to the conduction through the wick [9].

In order to avoid these inconveniences, this work presents the study of a wickless heat pipe applied to a TEG. Instead of using capillary effect, this device uses the thermosyphon effect, which takes advantage of density differences and gravity force to make the fluid flow inside the exchanger. It does not require any fan or pump to work; it just needs the evaporator to be below the condenser to allow the fluid drain back once it has been condensed. A thermosyphon with phase change (TSP) has -like a heat pipe- an evaporator, a vapor line, a condenser (composed by several finned tubes for the natural convection) and a liquid return line.

The main goal of this work is to design thermosyphons with phase change and study their performance as cold-side heat exchangers in TEGs, which, as they do not need any auxiliary consumption, could improve the net generation of electric energy.

For that, Section 2 describes a computational model that has been developed to predict the performance of thermosyphons with phase change. Section 3 presents a prototype designed, built and tested to prove the performance of these systems and to validate the model. Section 4 shows the experimental and simulated results obtained from the prototype and the computational model respectively. Section 5 presents a parametric study conducted for design and optimization of this kind of heat exchangers, and also a study of the improvement in the production of electricity using

TEGs for waste heat harvesting from a chimney. A comparison has been made between the use of finned dissipaters and thermosyphons as cold-side heat exchangers. Finally, Section 6 collects the main conclusions of this work.

2. Computational Model

To study the use of thermosyphons with phase change in thermoelectric generators is necessary to, firstly, develop a computational model able to predict the behaviour of these heat exchangers. The model must simulate their performance with enough accuracy and convergence rate, allowing the modification of dozens of parameters. This cannot be achieved using a CFD software [6], due to its high computational cost, even when modifying one single parameter. Because of that, the finite-differences implicit method has been employed, which has been proven to be useful in not only this kind of TEG applications [12] but also in those of thermoelectric refrigeration [13].

It has been also taken into account several phenomena that occur in TEGs, such as constriction and contact thermal resistances, and the disposition of the condenser tubes.

The finite-differences method requires the geometry of the device to be discretized, as Figure 1 displays. The thermal resistances that determine the heat transfer between all the nodes are obtained from the calculation of the boiling and condensation coefficients inside the evaporator and the tubes respectively, the heat conduction through the walls, and the constriction and contact thermal resistances. Then, the temperatures in the system can be calculated.

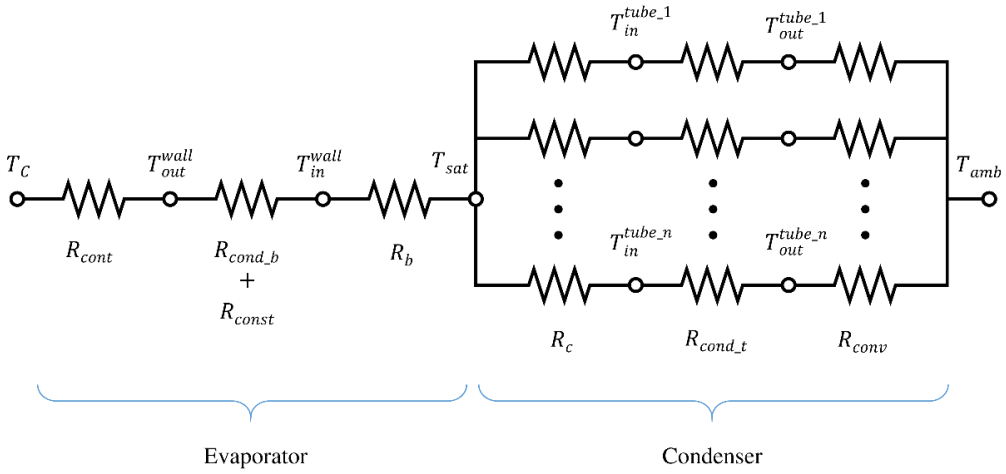

Figure 1. Thermal-electric analogy of the thermosyphon with phase change

Following the heat flux from the thermoelectric modules to the ambient, the first thermal resistance is the contact between the TEMs and the evaporator. The estimation of its value depends on the contact interface material that can be employed (contact grease, graphite sheets, etc.). Knowing the thermal conductivity, the base area and the thickness of the interface material used, the thermal contact resistance can be calculated with Eq. (1) [14]

$$R_{cont} = \frac{e_{im}}{k_{im} A_{im}} \tag{1}$$

Then, there is a heat conduction through the wall of the evaporator's base. This resistance is estimated according to Eq. (2) [14].

$$R_{cond\_b} = \frac{e}{k_{Al} A_b} \tag{2}$$

Furthermore, other phenomenon takes place in this wall: the constriction. This term describes the situation where the heat flows out of a narrow region, the TEMs, into a larger cross sectional area, the evaporator's base. In some cases, this constriction thermal resistance may be greater than the conduction resistance described above [15]. To estimate its value Eqs. (3)-(5) [15] are used.

$$R_{const} = \frac{\Psi}{k_{Al}\sqrt{A_m}} \tag{3}$$

where Ψ is the dimensionless constriction resistance, calculated according to Eq. (4) and A_m is the area of a thermoelectric module, with λ_c being an empirical parameter given by Eq. (5) and ϵ the dimensionless contact radius $(\sqrt{\delta})$.

$$\Psi = \frac{\tanh(\lambda_c \tau) + \frac{\lambda_c}{Bi}}{1 + \frac{\lambda_c}{Bi} \cdot \tanh(\lambda_c \tau)} \tag{4}$$

$$\lambda_c = \pi + \frac{1}{\sqrt{\pi}\,\epsilon} \tag{5}$$

After having crossed the evaporator's wall, the heat evaporates the refrigerant. To calculate the boiling resistance, a boiling coefficient must be estimated. The correlation here used was proposed by Forster and Zuber and is given by Eq. (6) [16].

$$h_b = \frac{0.00122 \Delta T_{sat}^{0.24} \Delta P_{sat}^{0.75} c_{pl}^{0.45} \rho_l^{0.49} k_l^{0.079}}{\sigma^{0.5} i_{lg}^{0.24} \mu_l^{0.29} \rho_g^{0.24}} \tag{6}$$

A correlation to estimate the heat transfer during condensation inside plain tubes has been employed. These expressions, proposed by Shah [17], are valid for tubes inclined downward less than 15°. The condensation transfer coefficient is obtained from a combination of Eqs. (7) and (8), depending in the regimen of the flow through the tubes. For turbulent flow regimen the first equation must be employed whereas for laminar regimens the second one is used.

$$h_{cI} = 0.023 Re_{LT}^{0.8} Pr_l^{0.4} \left(\frac{\mu_l}{14\mu_g}\right)^{(0.0058+0.0557 p_r)} \left[(1-x)^{0.8} + \frac{3.8 x^{0.76} (1-x)^{0.04}}{p_r^{0.38}}\right] \tag{7}$$

$$h_{cII} = 1.32 Re_{LS}^{-1/3} \left[\frac{\rho_l (\rho_l - \rho_g) g k_l^3}{\mu_l^2}\right]^{1/3} \tag{8}$$

Once the vapour has condensed inside the inclined tubes, the heat passes through the walls of those tubes and finally it is released to the ambient. The first mechanism is a heat conduction and it is estimated using Eq. (9) [14].

$$R_{cond\_t} = \frac{ln\left(\frac{d_e}{d_i}\right)}{2\pi k_{Al} L} \tag{9}$$

The natural convection between the finned tubes and the ambient has been calculated using the experimental correlation proposed by Tsubouchi and Masuda [18] for circular fins. As the fins in the prototype that will be studied later are square an equivalent diameter must be used, see Eq. (10) [18].

$$D = 1.23\,H \tag{10}$$

The heat transfer from the fins are correlated with Eq. (11), where Ra is the Rayleigh number given by Eq. (12), and γ and C_1 parameters calculated with Eqs. (13)-(14), with $\xi = d_e/D$.

$$Nu = \frac{Ra}{12\pi}\left\{2 - exp\left[-\left(\frac{C_1}{Ra}\right)^{3/4}\right] - exp\left[-\gamma\left(\frac{C_1}{Ra}\right)^{3/4}\right]\right\} \tag{11}$$

$$Ra = \frac{g\beta(T_w - T_{amb})S^3}{\nu\alpha}\cdot\frac{S}{D} \tag{12}$$

$$\gamma = 0.17\xi + e^{-4.8\xi} \tag{13}$$

$$C_1 = \left[\frac{23.7 - 1.1(1 + 152\xi^2)^{1/2}}{1+\gamma}\right]^{4/3} \tag{14}$$

With all these expressions the total thermal resistance of the heat exchanger can be calculated, which is the output of the computational model here presented.

3. Prototype

The prototype built to study the behaviour of the heat exchanger can be seen in Figure 2.The main elements, indicated in the figure, are: the evaporator, the vapour line, the condenser (compound by several finned tubes) and the liquid return line. They are held by an aluminium structure made up of bars and four legs. It also has a manometer and a safety valve that keeps the inside pressure under control.

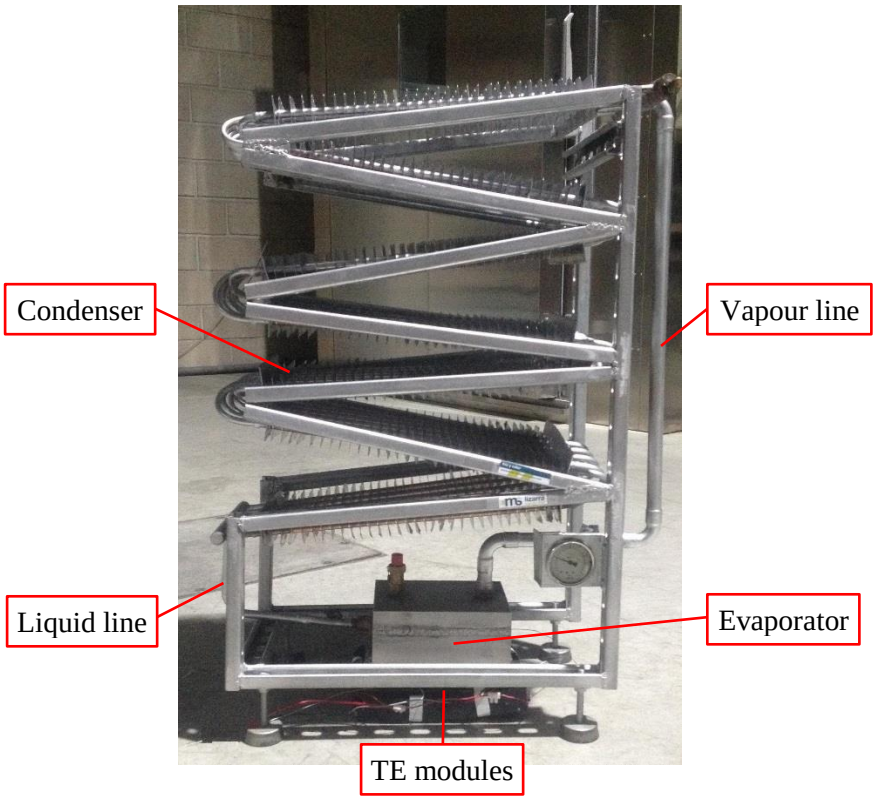

Figure 2. Prototype of the thermosyphon heat exchanger

The heat introduced to the exchanger, that needs to be dissipated, would come from the cold side of the thermoelectric modules that are placed on the lower side of the evaporator. For the experiments, plain electric resistances have been located in that part, in order to easily control the amount of heat that it is passed to the device. After going through the evaporator's wall, the heat introduced to the system warms the refrigerant inside up causing its evaporation. The vapour generated goes up through the vertical tube and, once it is on top of the exchanger, the flow is split into 6 tubes where the vapour condensates releasing the heat to the ambient. To help in this duty and to improve the natural convection between the dissipation system and the ambient, square fins are located on the condensation tubes. After the condensation, the liquid refrigerant returns to the evaporator due to gravitational forces.

All the main components of this system are made of aluminium and their dimensions are described in Table 1 and the refrigerant fluid employed is R-134a [19].

Table 1. Dimensions of the thermosyphon prototype

Thermosyphon zone	Parameter	Measurements
Evaporator		
Rectangular prism	Base	230 x 190 mm²
	Height	110 mm
	Wall thickness	3 mm
Vapour line	Length	640 mm
	Diameter	22 mm
Condenser		
Tubes	No. tubes	6
	Length (each)	3.5 m
	Diameter	10 mm
	Thickness	2 mm
Finns	Height	40 mm
	Width	40 mm
	Thickness	0.5 mm
	Fin spacing	12 mm

As explained before, the TEMs would be in charge of introducing the heat into the dissipation system. Instead of that, electric resistances, with a base area of 40 x 40 mm², are employed, being placed, evenly separated, in the base of the evaporator and connected to a Wayne Kerr AP10090 electric power supply. With this configuration the two factors examined here can be controlled. The occupancy ratio is the first factor. It is defined by Eq. (15) and represent the area that would be covered by the modules in relation to the total area available for the heat transfer, in this case the evaporator's base. The second factor is the heat power to be dissipated, which is controlled by the power source to which the electric resistances are connected.

$$\delta = \frac{N \cdot A_m}{A_b} \tag{15}$$

To ensure a good contact that allows a proper heat transfer between the electric resistances and the evaporator's base a metal plate is screwed to tighten the assembly. Furthermore, a graphite sheet is put between these resistances and the evaporator. This reduces the contact thermal resistance, which is key in these applications [20]. The graphite sheet has a thermal conductivity of 10 W/mK and a thickness of 0.127 mm [21].

In order to maintain the ambient conditions equal, all the experiments are made inside a climatic chamber that keeps the temperature at 22 °C.

The input variables in the experiments are: the temperature of the evaporator's base, T_c, the ambient temperature, T_{amb}, and the voltage, V_{ps}, and electric current, I_{ps}, supplied by the power source. Both temperatures (T_c and T_{amb}) are measured by Ahlborn T190-0 NiCr-Ni thermo-wires, which are connected to an Ahlborn Almemo 5690-1M09 data acquisition system.

After the calibration, the systematic uncertainties turn out to be respectively $b_T = 0.3\ °C$, $b_{V_{ps}} = 0.1\ V$ and $b_{I_{ps}} = 0.05\ A$.

With all these variables measured, the thermal resistance per module of the heat exchanger can be calculated according to Eq. (16). This is one of the main parameters under study in this paper and it is used to evaluate the thermal performance of the dissipation system.

$$R_{HE} = \frac{N \cdot (T_c - T_{amb})}{V_{ps} \cdot I_{ps}} \tag{16}$$

4. Results and Analysis

Once the prototype and the computational model have been presented, this section contains the results of the experimentation as well as the simulation values of the thermal resistance. With them, a validation of the computational model has been made.

4.1. Experimental and Computational Results

Four different values for the occupancy ratio and six for the power to be dissipated have been tested. However, due to the limit of the maximum electric power that can flow through the electric resistances employed in the prototype, some values, related to low occupancy ratios, have been omitted from the experiments. For the 15 different cases studied, three replicas have been reproduced. The ambient temperature, inside de climatic chamber, has been set constant along the

experiments. The parameters measured in the experiments were, as it was explained before, the temperature in the evaporator's base, the ambient temperature and the voltage and current supplied to the electric resistances, with which the power to be dissipated can be easily calculated with Eq. (17).

$$\dot{Q}_c = V_{ps} \cdot I_{ps} \tag{17}$$

After the experimentation the thermal resistance of the exchanger can be calculated using Eq. (16). The values of this parameter and the input variables are shown in Table 2. The overall uncertainty has been calculated too, based on Coleman's work [22]. This overall uncertainty is composed of the random standard uncertainty for the mean (three replicas of every scenario have been carried out) and the systematic standard uncertainty, which is calculated with Eqs. (18) and (19) for every parameter.

$$b_{\dot{Q}_c}^2 = I_{ps}^2 b_{V_{ps}}^2 + V_{ps}^2 b_{I_{ps}}^2 \tag{18}$$

$$b_{R_{HE}}^2 = \left(\frac{1}{I_{ps}V_{ps}}\right)^2 b_T^2 + \left(\frac{T_c - T_{amb}}{I_{ps}^2}\right)^2 b_{\dot{Q}_c}^2 = \left(\frac{1}{\dot{Q}_c}\right)^2 b_T^2 + \left(\frac{R_{HE}}{\dot{Q}_c}\right)^2 b_{\dot{Q}_c}^2 \tag{19}$$

Figure 3 depicts the heat exchanger thermal resistance per module obtained from both the simulations and the experimental tests, in function of the power that is dissipated for different values of the occupancy ratio. For the empirical results, the overall uncertainty range has been included. The model is deterministic, so no variation in the results is expected. It can be seen that the thermal resistance is dependent on both the occupancy ratio and the power. The thermal resistance decreases as the power to be dissipated get higher values, owing to the increase in the intermediate temperatures (saturation temperature of the refrigerant and wall temperatures) which causes an improvement of the heat transfer coefficients and thus a reduction in the values of the thermal resistance. Besides, an increase in the occupancy ratio provokes an increase in the values of the thermal resistance per module. Having higher values of the occupancy ratio means more modules in the same exchanger, which results in less dissipation area per module.

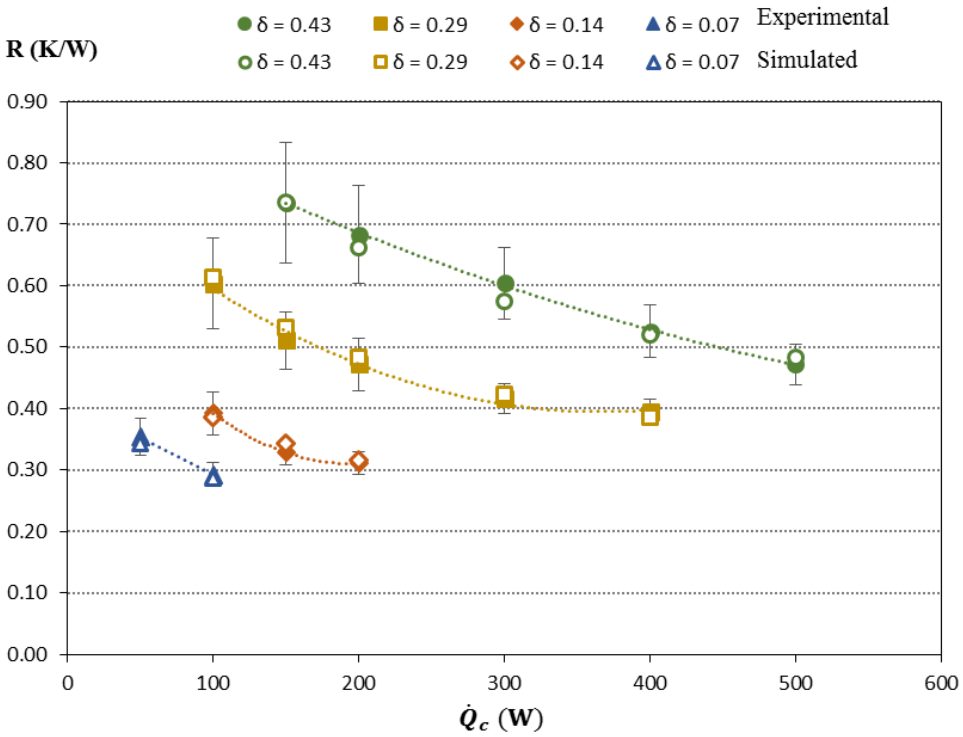

Figure 3. Thermal resistance of the heat exchanger dependence on the power dissipated for different occupancy ratios

4.2. Model Validation

The results of the simulation are shown as well in Table 2. The relative error between the simulated and experimental values of the thermal resistances is estimated through Eq. (20).

$$Relative\ error = \frac{Value_{exp} - Value_{sim}}{Value_{exp}} \cdot 100 \tag{20}$$

A statistical analysis can be made to the values of the relative error. This sample can be described as a normal distribution with mean -0.13 and standard deviation 4.06. Therefore, the model predicts the thermal resistance of the heat exchanger with a relative error in the interval [-8.09; 7.83] percent in the 95% of the cases. Besides, as it can be seen in Figure 4, all the relative errors are within the range ±9 %.

Table 2. Experimental and simulated results

Working point		Thermal Resistance (K/W)		
Occupancy ratio	**Power dissipated (W)**	**Exp.**	**Sim.**	**Error (%)**
0.07	50	0.35	0.34	1.97
		0.34		-0.12
		0.37		6.50
	100	0.28	0.29	-1.55
		0.29		-0.32
		0.31		5.92
0.14	100	0.38	0.39	-1.10
		0.38		-2.93
		0.42		7.31
	150	0.34	0.34	-1.59
		0.33		-3.47
		0.32		-8.13
	200	0.32	0.32	1.21
		0.31		-0.28
		0.30		-5.49
0.29	100	0.57	0.61	-7.21
		0.63		2.48
		0.61		-0.94
	150	0.52	0.53	-1.59
		0.51		-5.01
		0.50		-5.75
	200	0.45	0.48	-6.70
		0.49		2.05
		0.47		-2.70
	300	0.42	0.42	-1.65
		0.42		-1.03
		0.42		-1.68
	400	0.40	0.39	4.26
		0.39		1.87
		0.39		0.86
0.43	150	0.71	0.73	-3.36
		0.78		6.21
		0.71		-3.25
	200	0.68	0.66	2.88
		0.71		7.13
		0.65		-1.11
	300	0.62	0.57	7.78
		0.58		0.74
		0.61		6.08
	400	0.52	0.52	0.42
		0.51		-1.21
		0.54		3.76
	500	0.48	0.48	-1.63
		0.46		-5.08
		0.48		-0.60

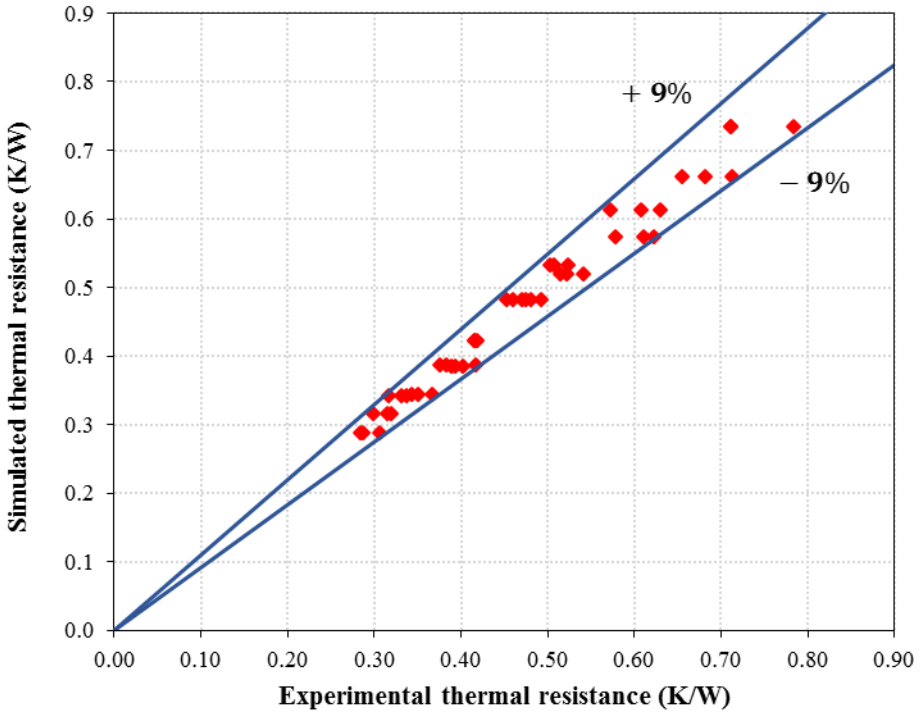

Figure 4. Thermosyphon simulated thermal resistance in the ±9 % experimental resistance range

The computational model has also a good convergence rate, being able to solve each case in less than 3 seconds. These facts together with its versatility make the model a good optimization tool for the heat exchanger design. As several geometry parameters can be modified and different configurations can be taken into account, it is easy now to study different thermosyphons heat exchangers with phase change trying to reduce their value of the thermal resistance. This would have an impact on the amount of electric power generated, when they are placed on the cold side of TEGs.

5. Thermosyphons with Phase Change Applied to TEGs

The final goal of this work is to assess the improvements of the use of thermosyphons heat exchangers with phase change in TEGs that are focused on the harvesting of waste heat from industrial processes. Having no auxiliary consumption, due to the lack of fans or pumps, these heat exchangers allow to make use of the whole electric power obtained from the TEG, in contrast

to traditional dissipaters, where part of the electricity produced must be employed to feed the dissipation system itself. That is why it is so crucial to calculate not only the total amount of electric power produced but also the net power generated [23].

To prove this enhancement, an analysis has been made comparing the use of this kind of passive dissipaters with common finned heat exchangers applied to a specific TEG. The case chosen here has been taken from a previous study [1], in which a TEG used the heat of the smoke from a paper mill's combustion boiler (temperature of the smoke: 200 °C) to produce electricity. In that study, the authors considered a 1 m duct height, with squared base area of 0.88 m (which corresponded to 3.52 m² of surface area) containing 320 TEMs. They provided Eq. (21) , with which the electric power generated could be estimated, just knowing the thermal resistances of the heat exchangers placed on both sides of the TEMs.

$$1/P_{max} = 0.00042018 + 0.000495173R_{hot} + 0.000809915R_{cold} + 0.000156221R_{hot}^2 + 0.000300105R_{hot}R_{cold} + 0.000495173R_{cold}^2 \quad (21)$$

The authors used two finned heat exchangers: one located in the hot side of the generator (inside the duct) with a thermal resistance of 0.338 K/W per installed TEM; and the other connecting the cold side of the TEMs and the ambient, with a thermal resistance of 0.523 K/W per module. They achieved to produce a total electric power of 821 W (about 233 W/m²), but, as the cold side dissipater required 150 W to operate some fans, the net electric power generation was of 671 W (191 W/m²).

The proposal here is to replace the outside finned dissipaters with thermosyphon heat exchangers with phase change, removing, in this sense, the necessity of a fan. For that, the thermal resistance of this passive heat exchanger is calculated with the model presented in this work, and the total electric power is estimated using Eq. (21).

Two configurations for the thermosyphon are proposed and compared to the previous study [1]. In order to provide valid comparisons, the occupancy ratio is set to 0.145, corresponding to 320

TEMs with base 40 x 40 mm^2 installed on 3.52 m^2 of chimney surface [1]. The heat exchanger in the hot side is also maintained, so a thermal resistance of 0.338 K/W is used in Eq. (20).

In the first configuration, sixteen thermosyphons similar to the prototype presented in section 3 have been selected, that is, four thermosyphons for each face of the chimney. The design has been modified in order for each thermosyphon to be able to dissipate the heat that comes from 20 TEMs (see that the prototype includes a maximum of 12 TEMs). So each one presents evaporator's base of 0.5 x 0.44 m^2 and an increased condenser area that includes 8 branches of tubes, 4 m long each, covered by 40 x 40 mm^2 square fins, 8 mm spaced. According to the computational model, this configuration leads to a thermal resistance per module of 0.65 K/W. Using this value in Eq. (21), the total electric power that could be generated would be of 711 W (202 W/m^2), lower than using finned dissipators. However, as this system does not require any auxiliary consumption, the net power is also 711 W, which is a 6 % higher.

For the second configuration, the design of the thermosyphon is improved in order to increase the net electric generation. To properly do so, a design-of-experiments-based statistical optimization has been carried out. This is one of the best optimization methods, because it gives the widest objective information with the smallest number of runs [24]. Statistical software Statgraphics has been used. The factors here considered are: occupancy ratio, evaporator's base thickness, condensation tube's length, fin's height and distance between them. A screening factorial design (resolution V+) was used, with a total of 32 runs. The low and high levels of each factor are specified in Table 3.

Table 3. Low and high levels of each factor in the screening factorial design

Factor	Low level	High level
A: Occupancy ratio	0.07	0.43
B: Evaporator's base thickness	5 mm	10 mm
C: Length of the condensation tubes	2 m	3 m
D: Height of the fins	20 mm	40 mm
E: Distance between fins	5 mm	10 mm

The thermal resistance per module is the response variable here considered and the goal is to minimize its value. The solution for the 32 runs have been calculated with the computational model. For each run, the ambient temperature was set to 22 ℃ and the power that needs to be dissipated was set equal to 300 W, which are the same conditions considered for the heat exchangers in the previous study [1]. The results are shown in Table 4 and the influence of every parameter can be checked in the Pareto diagram, Figure 5.

Table 4. Results for the 32 runs

Run	A Occupancy ratio	B Evaporator's base thickness (mm)	C Length of the condensation tubes (m)	D Height of the fins (mm)	E Distance between fins (mm)	Response Thermal Resistance (K/W)
1	0.07	5	2	20	5	0.41
2	0.07	5	2	20	10	0.44
3	0.07	5	2	40	5	0.29
4	0.07	5	2	40	10	0.31
5	0.07	5	3	20	5	0.35
6	0.07	5	3	20	10	0.37
7	0.07	5	3	40	5	0.26
8	0.07	5	3	40	10	0.27
9	0.07	10	2	20	5	0.38
10	0.07	10	2	20	10	0.42
11	0.07	10	2	40	5	0.26
12	0.07	10	2	40	10	0.27
13	0.07	10	3	20	5	0.32
14	0.07	10	3	20	10	0.34
15	0.07	10	3	40	5	0.23
16	0.07	10	3	40	10	0.24
17	0.43	5	2	20	5	1.76
18	0.43	5	2	20	10	1.97
19	0.43	5	2	40	5	1.02
20	0.43	5	2	40	10	1.10
21	0.43	5	3	20	5	1.37
22	0.43	5	3	20	10	1.49
23	0.43	5	3	40	5	0.83
24	0.43	5	3	40	10	0.86
25	0.43	10	2	20	5	1.75
26	0.43	10	2	20	10	1.95
27	0.43	10	2	40	5	1.01
28	0.43	10	2	40	10	1.08
29	0.43	10	3	20	5	1.36
30	0.43	10	3	20	10	1.47
31	0.43	10	3	40	5	0.82
32	0.43	10	3	40	10	0.85

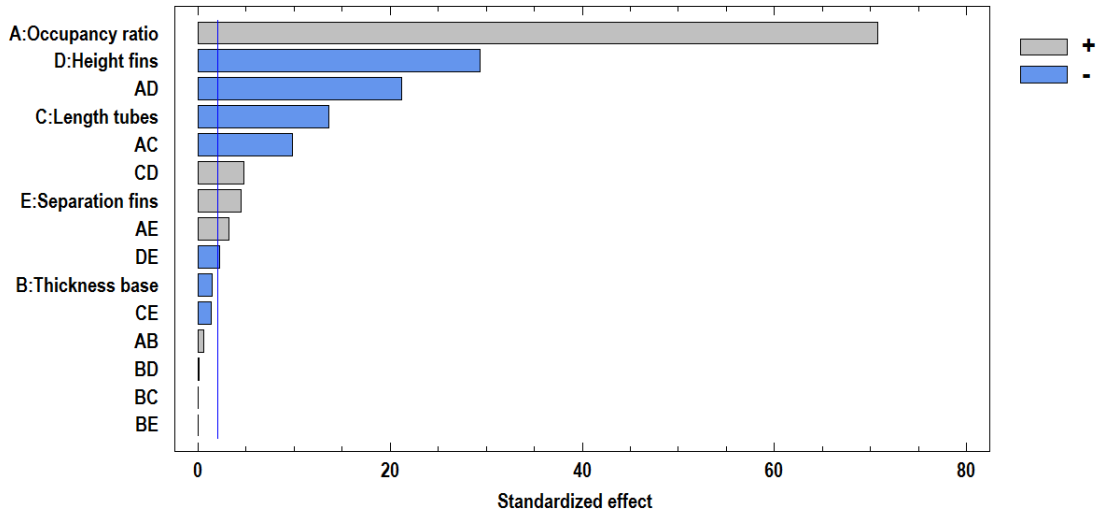

Figure 5. Pareto chart of effects on the thermal resistance

As expected, factor B (evaporator's base thickness) and its related interactions with other factors turn out not to be significant, with significance level of 0.05. Besides, the occupancy ratio is the most significant factor followed by the height of the fins and the length of the tubes, which correspond to the condenser part of the heat exchanger.

According to these results, the thermal resistance of this system can be decreased by an enhancement of the length of the tubes and the size of the fins, the most significant parameters after the occupancy ratio, which must be maintained equal to the value considered in the previous study. Increasing the length of the condenser tubes to 5 m, adding 2 more tubes to the branches and placing 50 x 50 mm^2 square fins, which is a 56 % more convective area, the thermal resistance per module decreases to a value of 0.44 k/W. In this new case, the total electric power that could be generated is 912 W (259 W/m^2), and, as it happened with the first configuration, there is no extra consumption. This represents an increase in 36 % of the net electric generation.

Figure 6 shows the comparison between these 3 cases that have been explained, revealing the importance of including the auxiliary consumption in the final estimations of the total electric power available from the thermoelectric generator.

The reduction of the cold side thermal resistances of the TEG would have an impact on its efficiency, since it causes an increase in the total electric power generated and would cause a rise

in the amount of heat absorbed from the smoke. But, as there is no way to calculate that heat absorbed, it is not possible to estimate the efficiency of the TEG. However, it has been already proven that an increase in the electricity generated implies an increment in that efficiency [23,25]. Consequently, an increase in the efficiency of the TEG is expected when using thermosyphons with phase change that reduce the thermal resistances of the cold side.

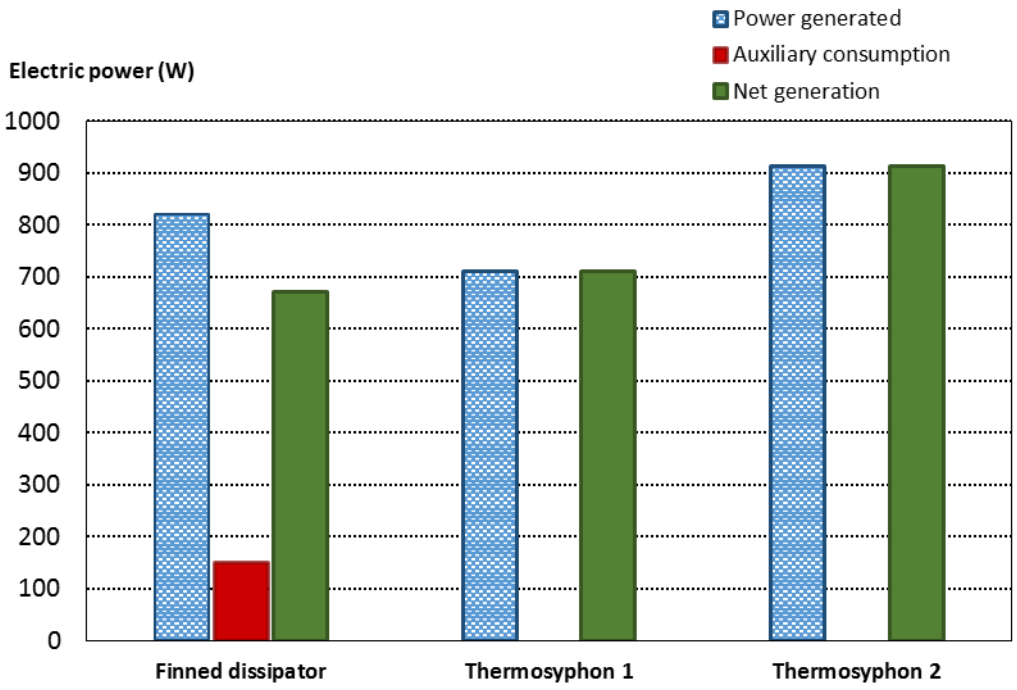

Figure 6. Comparative analysis using different cold side heat exchangers

6. Conclusions

A study of the use of passive heat exchangers based on the thermosyphon effect with phase change applied to thermoelectric generators has been accomplished. It has been developed a computational model that is able to predict the behaviour of this kind of heat exchangers. The way this model has been developed turns this software into a useful design tool, considering that several parameters can easily be modified and it takes few seconds to obtain a new solution.

A prototype has also been built to prove the performance of this passive systems. For that, several experiments have been carried out and some of the results have been employed in the validation

of the computational model. The maximum relative error between the simulated results and the experimental ones for the thermal resistance of the exchanger is lower than 9 %. Specifically, it turns out that the model predicts the thermal resistance of the heat exchanger with a relative error in the interval [-8.09; 7.83] percent in the 95% of the cases.

Finally, the use of this thermosyphons heat exchangers with phase change placed in the cold side of a TEG has been studied. The TEG analysed generates electricity using the waste heat that comes from the chimney of a boiler. This solution has been compared to a previous study in which finned dissipaters were employed as cold-side heat exchangers and where an extra electric consumption was required to feed the fans of the devices. This auxiliary power consumption decreases the net electric generation and, because of that, passive systems, as the thermosyphons with phase change presented here, turn out to be a real alternative. Besides, this kind of heat exchangers would reduce the maintenance of the whole system due to the lack of moving parts.

As it has been proven, using a thermosyphon with phase change with a higher thermal resistance (compared to the one of a finned dissipater) does not improve the total electric power generated, but it enhances the net generation, which is the useful electricity that can be employed at the end. Specifically, an increase of a 6 % in the net generation can be achieved.

Furthermore, the design of the thermosyphon can be improved by increasing the condensation area in order to get lower thermal resistances, and consequently, rise the electric power that can be obtained up to 912 W, that is 259 W/m², which represents a 36 % more than the net electric power generated using finned dissipaters.

7. Acknowledgements

The authors are indebted to the Spanish Ministry of Economy and Competitiveness and FEDER funds for economic support of this work, included in the DPI2014-53158-R Research Project.

8. References

[1] Astrain D, Vián JG, Martínez A, Rodríguez A. Study of the influence of heat exchangers' thermal resistances on a thermoelectric generation system. Energy 2010;35:602–10. doi:10.1016/j.energy.2009.10.031.

[2] He W, Wang S, Li Y, Zhao Y. Structural size optimization on an exhaust exchanger based on the fluid heat transfer and flow resistance characteristics applied to an automotive thermoelectric generator. Energy Convers Manag 2016;129:240–9. doi:10.1016/j.enconman.2016.10.032.

[3] Martinez A, Astrain D, Aranguren P. Thermoelectric self-cooling for power electronics: Increasing the cooling power. Energy 2016;112:1–7. doi:10.1016/j.energy.2016.06.007.

[4] Gou X, Xiao H, Yang S. Modeling, experimental study and optimization on low-temperature waste heat thermoelectric generator system. Appl Energy 2010;87:3131–6. doi:10.1016/j.apenergy.2010.02.013.

[5] Tzeng SC, Jeng TM, Lin YL. Parametric study of heat-transfer design on the thermoelectric generator system. Int Commun Heat Mass Transf 2014;52:97–105. doi:10.1016/j.icheatmasstransfer.2014.01.021.

[6] Aranguren P, Astrain D, Martínez A. Study of complete thermoelectric generator behavior including water-to-ambient heat dissipation on the cold side. J Electron Mater 2014;43:2320–30. doi:10.1007/s11664-014-3057-x.

[7] Kim TY, Negash AA, Cho G. Waste heat recovery of a diesel engine using a thermoelectric generator equipped with customized thermoelectric modules. Energy Convers Manag 2016;124:280–6. doi:10.1016/j.enconman.2016.07.013.

[8] Elghool A, Basrawi F, Ibrahim TK, Habib K, Ibrahim H, Idris DMND. A review on heat sink for thermo-electric power generation: Classifications and parameters affecting

performance. Energy Convers Manag 2017;134:260–77. doi:http://dx.doi.org/10.1016/j.enconman.2016.12.046.

[9] Shabgard H, Allen MJ, Sharifi N, Benn SP, Faghri A, Bergman TL. Heat pipe heat exchangers and heat sinks: Opportunities, challenges, applications, analysis, and state of the art. Int J Heat Mass Transf 2015;89:138–58. doi:10.1016/j.ijheatmasstransfer.2015.05.020.

[10] Remeli MF, Tan L, Date A, Singh B, Akbarzadeh A. Simultaneous power generation and heat recovery using a heat pipe assisted thermoelectric generator system. Energy Convers Manag 2015;91:110–9. doi:10.1016/j.enconman.2014.12.001.

[11] Huang BJ, Hsu PC, Tsai RJ, Hussain MM. A thermoelectric generator using loop heat pipe and design match for maximum-power generation. Appl Therm Eng 2015;91:1082–91. doi:10.1016/j.applthermaleng.2015.08.059.

[12] Rodríguez A, Vián JG, Astrain D, Martínez A. Study of thermoelectric systems applied to electric power generation. Energy Convers Manag 2009;50:1236–43. doi:10.1016/j.enconman.2009.01.036.

[13] Martínez A, Astrain D, Rodríguez A, Aranguren P. Advanced computational model for Peltier effect based refrigerators. Appl Therm Eng 2016;95:339–47. doi:10.1016/j.applthermaleng.2015.11.021.

[14] Chapman AJ. Heat transfer. 4th ed. Macmillan; 1984.

[15] Lee S, Song S, Au V, Moran KP. Constriction/spreading resistance model for electronics packaging. Proc 4th ASME/JSME Therm Eng Conf 1995;4:199–206.

[16] Foster HK, Zuber N. Bubble dynamics and boiling heat transfer. AIChE J 1955;1:531–5.

[17] Shah MM. An Improved and Extended General Correlation for Heat Transfer During Condensation in Plain Tubes. HVAC&R Res 2009;15:5:889–913. doi:10.1080/10789669.2009.10390871.

[18] Tsubouchi T, Masuda H. Natural convection heat transfer from horizontal cylinders with circular fins. Fac Technol Tohokugakin Univ, Sendai, Japan 1970.

[19] Lemmon EW, McLinden MO, Friend DG. Thermophysical Properties of Fluid Systems. In: P. J. Linstrom, W. G. Mallard, editors. NIST Stand. Ref. Database Number 69, Gaithersburg MD: National Institute of Standards and Technology; n.d.

[20] Omer SA, Infield DG. Design optimization of thermoelectric devices for solar power generation. Sol Energy Mater Sol Cells 1998;53:67–82. doi:10.1016/S0927-0248(98)00008-7.

[21] GrafTech International. Graphite Pad HT-1205. [Online] 2016. http://www.graftech.com/wp-content/uploads/2014/12/TDS318-HITHERM.pdf.

[22] Coleman HW, Steele WG. Experimentation, Validation and Uncertainty Analysis for Engineers. 3ª. John Wiley & Sons; 2009. doi:10.1017/CBO9781107415324.004.

[23] Aranguren P, Astrain D, Rodríguez A, Martínez A. Experimental investigation of the applicability of a thermoelectric generator to recover waste heat from a combustion chamber. Appl Energy 2015;152:121–30. doi:10.1016/j.apenergy.2015.04.077.

[24] Montgomery DC. Design and analysis of experiments. Hoboken, NJ: 2005.

[25] Wang Y, Li S, Zhang Y, Yang X, Deng Y, Su C. The influence of inner topology of exhaust heat exchanger and thermoelectric module distribution on the performance of automotive thermoelectric generator. Energy Convers Manag 2016;126:266–77. doi:10.1016/j.enconman.2016.08.009.